# Polarized NEXAFS Spectroscopic Studies of Poly(butylene terephthalate), Poly(ethylene terephthalate), and Their Model Compounds

**Toshihiro Okajima* and Kazuyoshi Teramoto**

*Advanced Technology R&D Center, Mitsubishi Electric Corporation, 8-1-1, Tsukaguchi-Honmachi, Amagasaki, Hyogo 661-8661, Japan*

**Ryuichi Mitsumoto, Hiroshi Oji, Yasushi Yamamoto, Ikuko Mori, Hisao Ishii, Yukio Ouchi, and Kazuhiko Seki**

*Department of Chemistry, Graduate School of Science, Nagoya University, Furo-cho, Nagoya 464-8602, Japan*

*Received: February 17, 1998; In Final Form: May 27, 1998*

Near edge X-ray absorption fine structure (NEXAFS) spectra were obtained using total electron yield detection for poly(butylene terephthalate) (PBT) and poly(ethylene terephthalate) (PET) and their model compounds 4,4′-biphenyldicarboxylic acid dimethyl ester (PAM), 4,4′-biphenyldicarboxylic acid (PCA), and terephthalic acid (TPA). The spectra of PBT and PET were interpreted with the comparison of the spectral features of model molecules and the polarized NEXAFS spectra of oriented films of PAM, PCA, and PBT. From the polarization dependence, the peaks previously ascribed to a C 1s → $\pi^*$(ring) or $\pi^*$(ring/C═O) excitation at 289.8 eV and an O 1s → 3p/Rydberg or → $\pi^*$(C═O) transition at 536.4 eV were reassigned to a C 1s → $\sigma^*$(O−$CH_x$) transition and an O 1s → $\sigma^*$(O−$CH_x$) transition, respectively. The present results demonstrate that the polarization dependence of the NEXAFS spectra of oriented small analogous molecules are useful for the assignment of the NEXAFS spectra of polymers.

## 1. Introduction

Near edge X-ray absorption fine structure (NEXAFS) spectroscopy, also known as X-ray absorption near edge structure (XANES) spectroscopy, is a recently developed branch of X-ray spectroscopy, which is useful as a new tool of basic studies on material characterization and also as an analytical technique for chemical specification.[1] For polymers, NEXAFS offers information about the identification of the polymeric chain and the functional groups, their orientation, and also the unoccupied electronic structures both in the bulk and at the surface.[2−18] Also the characterization of polymers using NEXAFS in the field of micro-NEXAFS and organic reaction is rapidly growing.[19−21] In these studies, it is critically important to make correct interpretation of the spectra of fundamental polymers, since they form the basis for interpreting the spectra of more complex polymers.

The relationship between core excitation spectral features and the geometric and electronic structure of polymers has been explored by quantum chemical calculations and experimental studies. In principle core excitation spectra can be predicted by ab initio[22,23] or semiempirical quantum chemical calculations[24−27] of various degrees of sophistication. However, it is still impossible to make reliable assignments only with these calculations, and the experimental approach is indispensable.

One of the typical experimental approaches is the comparison with the spectra of related compounds. Often the "building block" principle[1] is employed, in which the spectrum of a polymer is regarded to be composed of the spectra of its constituent parts such as the monomer or other suitable molecular analogues. Besides the NEXAFS spectra, the core excitation spectra obtained by inner-shell electron energy loss spectroscopy (ISEELS)[28] are also used for such comparison. Another important experimental approach is the examination of the polarization dependence of the spectra of oriented molecules using polarized synchrotron radiation. In organic materials, the 1s level is the only core level for the major constituent elements C, N, O, and F. The excitation from a 1s level is allowed only when (1) the final state has p character at the excited atom and (2) the electric vector ***E*** of the incident X-ray has a parallel component to the axis of the p orbital. These selection rules are useful for assigning the spectral features when one can prepare an oriented sample.[1,4,13,29]

For the spectral assignments of polymers, the use of molecular analogues is particularly useful. First, their molecular geometries are often known, and their electronic structure can be calculated with reliable structural information. By examining a series of molecules of different conformations, even the conformational dependence can be examined. Second, the specimens of these molecules can be often prepared with much better degree of orientation than the oriented polymeric specimens, which are prepared by techniques such as elongation or surface rubbing. We have demonstrated this point for various polymers such as polyethylene,[4] poly(tetrafluoroethylene),[4,12] and poly(*p*-phenylene).[13]

In this study, we report C K-edge and O K-edge NEXAFS studies of poly(butylene terephthalate) (PBT), poly(ethylene terephthalate) (PET), and their molecular analogues. PBT is widely used in industry as electronic parts and has a similar molecular structure to PET, which is a typical engineering plastic. Recently the NEXAFS and ISEELS spectra of PET and related molecules have been extensively studied. The spectra of PET itself has been reported by several groups,[14−18] including biaxially elongated ones.[16] The ISEELS spectra of small related molecules in the vapor phase were measured, and

S1089-5639(98)01164-5 CCC: $15.00 
Published on Web 08/14/1998

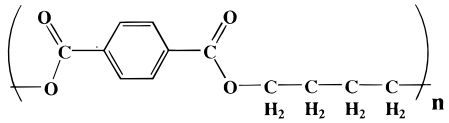

(a) Poly(butylene terephthalate) (PBT)

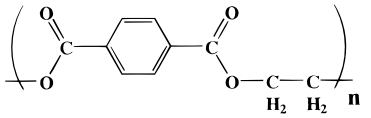

(b) poly(ethylene terephthalate) (PET)

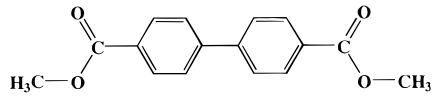

(c) 4,4'-Biphenyldicarboxylic Acid Dimethyl Ester (PAM)

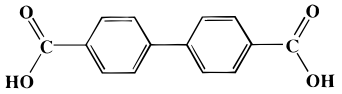

(d) 4,4'-Biphenyldicarboxylic Acid (PCA)

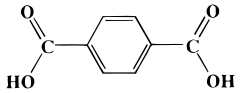

(e) Terephthalic Acid (TPA)

**Figure 1.** Molecular structures of (a) poly(butylene terephthalate) (PBT), (b) poly(ethylene terephthalate) (PET), (c) 4,4′-biphenyldicarboxylic acid dimethyl ester (PAM), (d) 4,4′-biphenyldicarboxylic acid (PCA), and (e) terephthalic acid (TPA). (c)−(d) are model compounds of PBT and PET.

theoretical calculations of the state of the art have been performed for these molecules.[14,17,18] However, there are still some ambiguity about the spectral assignments.

In this work, we aimed to reexamine these spectral assignments and solve the remaining ambiguity by the use of new model compounds. The molecular analogues used were 4,4′-biphenyldicarboxylic acid dimethyl ester (PAM), 4,4′-biphenyldicarboxylic acid (PCA), and terephthalic acid (TPA). The molecular structures of PET, PBT, and these molecules are shown in Figure 1. The observed spectral features were assigned by (1) the comparison among the observed spectra and, in particular, (2) the use of polarization dependence for well-oriented specimens of the model compounds as well as moderately oriented PBT. The well-oriented model compounds actually exhibited clear polarization, and new assignments are given to several features.

Together with the work of previous workers, this offers an example of how detailed assignments can be reached for the whole spectrum of fundamental polymers by the combination of various experimental and theoretical methods.

## 2. Experimental Section

PBT and PET without additives used in this study were commercially obtained from Teijin Limited. Their thin films were spin-coated onto Si(100) wafers with a 1 wt % solution of PBT and PET in 1,1,1,3,3,3-hexafluoro-2-propanol at 4000 revolutions/min. Examination of these films by X-ray photoelectron spectroscopy revealed the absence of an F 1s peak,

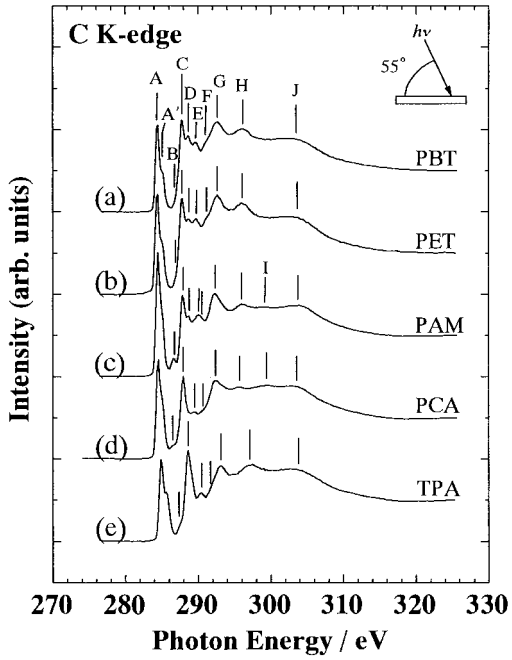


**Figure 2.** C K-edge NEXAFS spectra of PBT, PET, and related molecules at an X-ray incidence angle of 55°: (a) PBT, (b) PET, (c) PAM, (d) PCA, and (e) TPA. Note that peak D does not appear in the spectra of PCA and TPA, and peak I does not appear in the spectra of PBT, PET, and TPA.

confirming that the solvent was completely removed from the cast film by evaporation. The samples of PAM, PCA, and TPA were commercially obtained from Wako Pure Chemical Industry Ltd. and were used without further purification. The thin films of PAM and PCA were prepared by vacuum deposition onto Si(100) wafer at room temperature under vacuum of the $10^{-3}$ Pa range. The film thicknesses were about 150 nm. The sample of TPA was prepared by scrubbing the sample powder on a scratched copper plate. We also prepared a thin film of TPA by spin-coating onto Si(100) wafer with a 1 wt % solution of TPA in pyridine. However, we could not measure the NEXAFS spectra of this TPA film because the film sublimed away in a vacuum chamber before the NEXAFS measurements could be performed.

C K-edge and O K-edge NEXAFS spectra were measured at the soft X-ray beamline 11A of Photon Factory at National Institute for High Energy Physics. Synchrotron radiation from the storage ring was monochromatized by a Grasshopper monochromator with a grating of 2400 lines/mm.[30,31] The total energy resolution was estimated to be about 0.3 eV in the C K-edge NEXAFS region and 0.5 eV in the O K-edge region. Monochromatized X-rays were introduced into the measurement chamber with a base pressure of $10^{-6}$ Pa, and the NEXAFS spectra were obtained in the total electron yield mode. A metal grid coated with evaporated gold was inserted into the optical path, and the photon flux was monitored as the hole drain current $I_0$ from this grid by a picoammeter. The emitted electrons from the sample surface were collected and amplified by a channeltron, and the resultant current $I_S$ was measured by another picoammeter. The signal from each picoammeter was converted to a train of pulses by a $V-F$ converter, counted, and sent to a personal computer. The NEXAFS spectrum was obtained as $I_S/I_0$ vs photon energy.

The specimen was mounted so that it could be rotated around a vertical axis to change the incidence angle $\theta$ of the X-ray relative to the substrate surface from glancing angle ($\theta = 20°$)

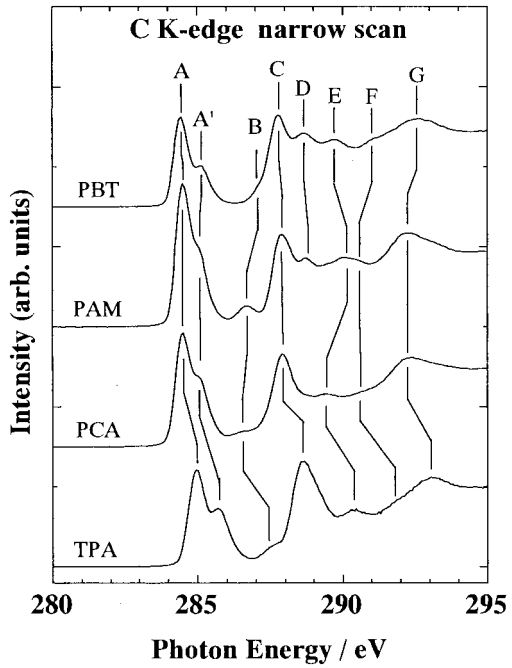


**Figure 3.** Comparison of the C K-edge NEXAFS spectra in the low photon energy region.

to normal incidence ($\theta = 90°$). The photon energy was calibrated using hexatriacontane ($n$-$CH_3(CH_2)_{34}CH_3$) in the C K-edge region and potassium sulfate ($K_2SO_4$) in the O K-edge region in standard materials, which were calibrated using the vapor spectra of Ar,[32] $N_2$,[33] $O_2$,[34] and $SF_6$.[35] The higher energy component of the lowest energy doublet peak of hexatriacontane was taken to be at 287.8 eV,[36] while the main peak energy of $K_2SO_4$ at the O K-edge was taken to be at 536.9 eV.[36] The resultant energy scale, when compared with those of other works on PET-related compounds, agrees with that in ref 16 but shows a 0.4 eV difference from that in ref 17. The origin of this deviation is not clear at present.

X-ray diffraction measurements were carried out at room temperature on the PAM and PCA thin films, using a Rigaku RAD-rC system. A conventional $\theta-2\theta$ scanning technique in the symmetrical reflection mode was used, with Cu K$\alpha$ radiation and a graphite monochoromator.

The ground-state molecular structure of PAM was provided by a semiempirical geometry optimization with the modified neglect of diatomic overlap-parametric method 3 (MNDO-PM3)[37] using the program MOPAC version 6.[38]

## 3. Results and Discussion

**A. C K-Edge NEXAFS Spectra.** Figure 2 shows the C K-edge NEXAFS spectra of (a) PBT, (b) PET, (c) PAM, (d) PCA, and (e) TPA at an X-ray incidence angle of $\theta \sim 55°$ (so-called magic angle[1,29]). At this incidence angle, possible effects of preferred molecular orientation can be removed.[1,29] Figure 3 shows the expanded spectra in the low photon energy region corresponding to the C 1s $\rightarrow \pi^*$ excitations. The spectrum of PET was almost identical to that of PBT. The spectra of these compounds are fairly similar, but there are also differences. First, the peak D appearing in the spectra of PBT, PET, and PAM does not appear in those of PCA and TPA. Second, peak I appearing in the spectra of PAM and PCA does not appear in those of PBT, PET, and TPA. The energies and proposed assignments of the features are listed in Table 1, together with the assignments about PET by other workers.

We start the detailed assignments from the examination of the polarization dependence. In parts a, b, and c of Figure 4, the C K-edge NEXAFS spectra of PBT, PAM, and PCA are shown as functions of the X-ray incidence angle $\theta$, respectively. All the sets of spectra show dependence on $\theta$, indicating the successful preparation of oriented films. On the other hand, the spectra of PET film and TPA powder showed little $\theta$-dependence. A high degree of orientation in evaporated films of molecular materials has also been observed for other compounds such as alkanes,[4] perfluoroalkanes,[4,12] and aromatic hydrocarbons.[39] We note that simple spin-coating of PBT still gave a reasonably oriented film. This is in contrast to the case of PET, where even biaxial elongation did not give well-oriented films.[16]

The $\theta$-dependence is most clearly seen in the spectra of PAM, where the peaks A, A′, B, C, E, and F are strongest at normal incidence ($\theta = 90°$), while they become weak with decreasing $\theta$. Other peaks D, G, H, I, and J show the opposite trend. In the spectra of PBT and PCA, on the other hand, peaks A, A′, B, C, E, and F are strongest at the grazing incidence ($\theta = 20°$), while they become weak with increasing $\theta$. Peaks D, G, H, and I show decreasing intensity with $\theta$. These trends are just the opposite of those for PAM.

In Figure 5, the X-ray diffraction pattern of PAM thin film on Si(100) wafer is shown. The observed reflections can be well-explained with a single interplanar spacing of about 1.5 nm, which is close to the length of the long axis of a molecule of PAM in the optimized geometry shown in Figure 6. This shows that the PAM molecules are oriented with their long axis vertical to the substrate, with the plane of the benzene ring

**TABLE 1: Experimental Energies (eV), Assignments, and Polarization Dependence for Features in the C K-Edge NEXAFS Spectra of Poly(ethylene terephthalate) (PET), Poly(butylene terephthalate) (PBT), and Its Model Compounds, 4,4′-Biphenyldicarboxylic Acid Dimethyl Ester (PAM), 4,4′-Biphenyldicarboxylic Acid (PCA), and Terephthalic Acid (TPA), and Comparison of the Assignments of Features between the Results of This Work and Those of Previous Papers[16,17]**

| | this work | | | | | | | ref 17 | | ref 16 | | |
|---|---|---|---|---|---|---|---|---|---|---|---|---|
| | energy (eV) | | | | | polarization | | energy | | energy | polarization | |
| feature | PET | PBT | PAM | PCA | TPA | dependence | assignment | (eV) | assignment | (eV) | dependence | assignment |
| A | 284.4 | 284.4 | 284.5 | 284.5 | 285.0 | $\pi$ | $\pi^*$(ring) | 284.8 | $\pi^*$(ring) | 284.4 | $\pi$ | $\pi^*$(ring) |
| A′ | 285.1 | 285.1 | 285.0 | 285.0 | 285.7 | $\pi$ | $\pi^*$(ring) | 285.45 | $\pi^*$(ring) | | $\pi$ | $\pi^*$(ring) |
| B | 287.0 | 287.0 | 286.7 | 286.7 | 287.5 | $\pi$ | $\pi^*$(ring) | 287.4 | $\sigma^*$(C−H) | | | |
| C | 287.8 | 287.8 | 287.9 | 287.9 | 288.6 | $\pi$ | $\pi^*$(C═O) | 288.27 | $\pi^*$(C═O) | 287.8 | $\pi$ | $\pi^*$(C═O) |
| D | 288.7 | 288.7 | 288.8 | | | $\sigma$ | $\sigma^*$(O−$CH_x$) | 289.0 | $\pi^*$(ring/C═O) | 289.1 | | $\sigma^*$(C−H) |
| E | 289.8 | 289.8 | 290.1 | 289.4 | 290.4 | $\pi$ | $\pi^*$(ring) | 290.1 | $\pi^*$(C═O) | 289.7 | $\pi$ | $\pi^*$(ring) |
| F | 291.0 | 291.0 | 290.6 | 290.6 | 291.8 | $\pi$ | $\pi^*$(C═O) | | | | | |
| G | 292.7 | 292.7 | 292.2 | 292.2 | 293.1 | $\sigma$ | $\sigma^*$ | 292.8 | $\sigma^*$ | | $\sigma$ | $\sigma^*$ |
| H | 296 | 296 | 296 | 296 | 297 | $\sigma$ | $\sigma^*$ | 296.4 | $\sigma^*$ | | $\sigma$ | $\sigma^*$ |
| I | | | 299 | 299.5 | | $\sigma$ | $\sigma^*$(ring−ring) | | | | | |
| J | 303 | 303 | 304 | 303.4 | 303 | $\sigma$ | $\sigma^*$ | 303.3 | $\sigma^*$ | | $\sigma$ | $\sigma^*$ |

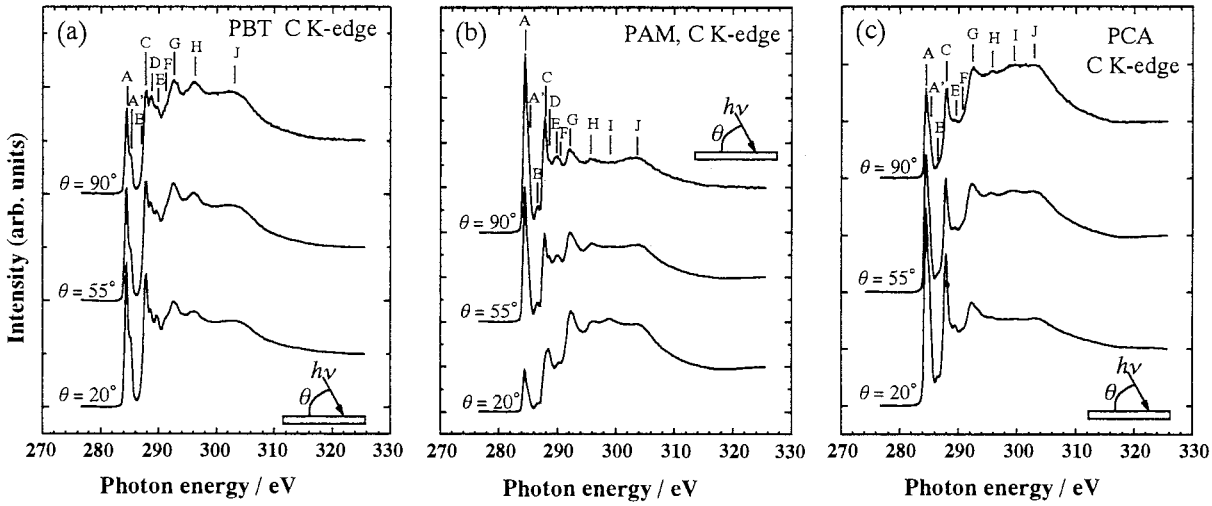


**Figure 4.** Polarization dependence of the C K-edge NEXAFS spectra of (a) PBT, (b) PAM, and (c) PCA on the X-ray incidence angle, $\theta$, relative to substrate surface.

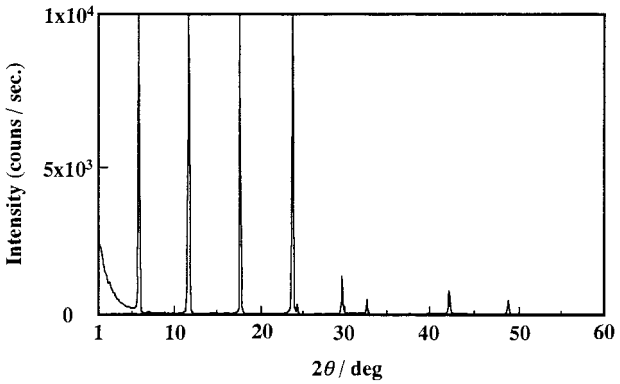


**Figure 5.** X-ray diffraction profile ($\theta-2\theta$ method) of PAM thin film on Si wafer. The sharp diffraction peaks correspond to a lattice spacing of 1.5 nm.

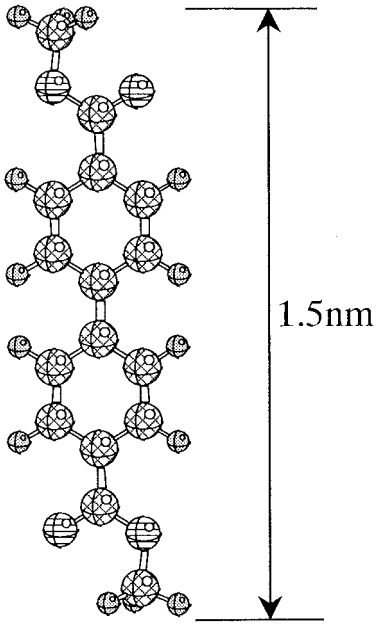


**Figure 6.** Optimized molecular structure of PAM calculated by the MNDO-PM3 method. The upper half consists of (i) the phenyl ring and the COOC part of the ester group in a plane and (ii) the three H atoms in the methyl group. The lower half also has the same structure. The angle between the planes of the upper and lower halves is 66.2°.

almost parallel to the surface normal. PCA thin film also showed X-ray diffraction peaks, but not those corresponding to the standing molecular orientation as seen for PAM. Since the assignments of these observed peaks of PCA are not clear at present, X-ray diffraction does not offer definite information about the orientation of PCA molecules. However, the opposite $\theta$-dependence of the NEXAFS spectra of PCA to that of PAM indicates that the molecular long axis is parallel to the substrate. On the basis of this structural information, the observed polarization dependence can be easily interpreted.

As stated above, it is known that the absorption intensity from a 1s level is largest for ***E*** along the axis of the 2p atomic orbital forming the $\pi^*$ or $\sigma^*$ orbital, while it becomes zero for ***E*** perpendicular to the axis. In a planar $\pi$-conjugated system, the $\pi^*$ orbitals are composed of $2p_z$ orbitals, which are perpendicular to the plane. Thus an excitation to a $\pi^*$ orbital is allowed for ***E*** vertical to the molecular plane. On the other hand, $\sigma^*$ excitations localized in a $\sigma$ bond becomes allowed when ***E*** becomes parallel to the bond, which is in the molecular plane. Therefore the $\pi^*$ and $\sigma^*$ excitations are expected to show opposite dependence on $\theta$.

For vertically standing PAM molecules, the excitations to the $\pi^*$ orbitals will be strong for normal incidence, while they will be weak for grazing incidence. On the other hand, the $\sigma^*$ excitations will appear at both normal and grazing incidences. From the $\theta$-dependence of the spectral features of PAM, we can assign the peaks A, A′, B, C, E, and F to $\pi^*$ excitations and D, G, H, I, and J to $\sigma^*$ excitations. This is in agreement with the well-established assignment that the peak A in the spectrum of PET is due to the $\pi^*$ excitation in the benzene ring.[14−18] As seen later, such estimation of molecular orientations is also supported by the polarization dependence of the O K-edge spectra.

The $\theta$-dependence of the spectra of PBT and PCA can be interpreted with the same peak assignments, but assuming that the planes of benzene rings are almost parallel to the substrate surface.

After establishing the distinction between the $\pi^*$ and $\sigma^*$ excitations, we will discuss the peak assignments in more detail. We also refer the assignments by other workers, i.e., (a) the extensive comparison with the ISEELS spectra of analogous molecules, (b) extended Hückel molecular orbital (EHMO) calculations in the equivalent core approximation,[14] (c) ab initio calculations based on improved virtual orbital method on analogous molecules,[17] and (d) the examination of biaxially elongated film of PET.[16]

In the lowest energy region of the spectra in Figures 2 and 3, we see the dominating sharp peak A accompanied by a shoulder (A′) on the high-energy side. These features were assigned to C 1s(C−H) → $\pi^*$(ring) transitions to the LUMO and next LUMO, which are split from the doubly degenerate $\pi^*$ LUMO of benzene owing to the symmetry reduction and chemical shifts associated with the substitution of benzene ring by the ester group.

A small peak B is observed on the low-energy side of the intense peak C. The peak was assigned to a C 1s(C−R) → $\pi^*$(C═C) transition by the EHMO calculation[14] and a C 1s-($CH_x$) → $\sigma^*$(C−H) transition by the result of ab initio calculation.[17] Since this peak shows the same polarization dependence with peak A, the assignment to a C 1s(C−R) → $\pi^*$(C═C) transition is more plausible, although $\sigma^*$(C−H) excitation may also contribute to this feature.[18,39]

The second intense peak C was assigned to a C 1s(C═O) → $\pi^*$(C═O) transition, which is characteristic of an ester or carboxylic carbon.[14−18] Here the $\pi^*$(C═O) transition has the in-phase relationship of the two contributing $\pi^*$(C═O) portions. This assignment is consistent with the present results.

At the higher energy side of peak C, two small peaks D and E are observed in the spectra of PBT, PET, and PAM, while only one peak E is observed in those of PCA and TPA. The peak D was assigned to C 1s(C−R) → $\pi^*$(ring) excitation by EHMO calculation,[14] C 1s(C−H) → $\pi^*$(ring)/(C═O) excitation by ab initio calculation,[17] and C 1s → $\sigma^*$(C−H) excitation.[16] Peak E was assigned to C 1s → $\sigma^*$(C−C) excitation by EHMO calculation,[14] C 1s → $\pi^*$(C═O) excitation by ab initio calculation,[17] and C 1s → $\pi^*$(ring) excitation.[16] Here the $\pi^*$(C═O) excitations in the two parts have the out-phase relationship.

As described above, the polarization dependence of peaks D and E shows that they correspond to $\sigma^*$ and $\pi^*$ excitations, respectively. Also we note the difference among the molecular structures that PBT, PET, and PAM have O−$CH_x$ bonds in the molecule, while PCA and TPA do not. The peak D appears only in the spectra of molecules containing O−$CH_x$ bonds. From these results, we assign the peak D to a C 1s (O−$CH_x$) → $\sigma^*$-(O−$CH_x$) excitation.

As for peak E, we note that there are several reports about the NEXAFS spectrum of benzene, which ascribe the peak at around 289 eV to the second weak $\pi^*$ transition.[16,40] This should correspond to the C 1s(C−H) → $\pi^*$(ring/C═O) transition by ab initio calculation, which was previously ascribed to the peak D.[17] Therefore, we assign peak E to this C 1s(C−H) → $\pi^*$(ring/C═O) excitation.

We can also see a weak peak F at the lower energy side of peak G in the spectra of PBT and PET. This peak is not clear in the spectra of the model compounds. Its polarization dependence shows its $\pi^*$ character. The C 1s(C═O) → $\pi^*$-(C═O) transition predicted by ab initio calculation, which was previously ascribed to peak E,[17] may correspond to this peak F. Here the $\pi^*$(C═O) transition has the out-phase relationship.

The peaks G, H, and J cover broad $\sigma^*$ resonances attributed to the C═C(ring), C−C, C═O, and C−O bonds.[14−18]

Peak I appears only in the spectra of PAM and PCA containing a C−C bond between the two benzene rings. This suggests that this peak corresponds to the C 1s → $\sigma^*$(C−C, ring−ring) transition. To support this assignment, a similar peak was also observed in the NEXAFS spectra of *p*-terphenyl $C_6H_5$−$C_6H_4$−$C_6H_5$, which contains C−C bonds among the benzene rings.[39]

The high-energy excitations such as G − J, however, in most cases are mixed with other contributions such as multiple scattering[34,41,42] and extended X-ray absorption fine structure (EXAFS). Thus it is not certain whether we can assign them uniquely to specific transitions.

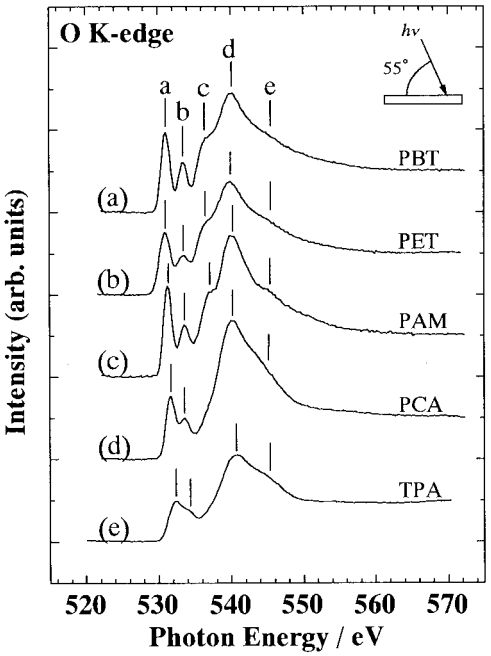


**Figure 7.** Comparison of the O K-edge NEXAFS spectra of PBT, PET, and related molecules at an X-ray incidence angle of 55°: (a) PBT, (b) PET, (c) PAM, (d) PCA, and (e) TPA. Note that peak c does not appear in the spectra of PCA and TPA.

**B. O K-Edge NEXAFS Spectra.** The O K-edge NEXAFS spectra of (a) PBT, (b) PAM, (c) PCA, and (d) TFA at $\theta \sim 55°$ are shown in Figure 7. The spectra are fairly similar, although there are also differences discussed later. The energies and proposed assignments of the features in the O K-edge NEXAFS spectra of PET, PBT, PAM, PCA, and TPA are listed in Table 2 along with the energies and assignments for PET by other workers.

In Figure 8a,b,c, the polarization dependence of the O K-edge spectra of PBT, PAM, and PCA are shown. In the spectrum of PAM, the intensities of the peaks a and b are strongest at normal incidence ($\theta = 90°$), while they become weak with decreasing $\theta$. Other peaks c, d, and e show the opposite trend. Since the results of X-ray diffraction for PAM film indicate that the plane of benzene ring is almost parallel to the surface normal, the present results indicate that the former and the latter groups mentioned above correspond to the $\pi^*$ and $\sigma^*$ excitations, respectively. This is in agreement with the established assignment that the lowest energy peak a correspond to the O 1s → $\pi^*$ transitions at the carbonyl oxygen.[14−18]

In the spectra of PBT and PCA, on the other hand, the intensities of peaks a and b are strongest at the grazing incidence ($\theta = 20°$), while they become weak with increasing $\theta$. Peaks c, d, and e show the opposite trend of decreasing intensity with $\theta$. These trends can be explained with the same peak assignments assuming flat-lying molecular orientation estimated from C K-edge spectra.

All the spectra in Figures 7 and 8 are dominated by the two intense peaks a and b at low photon energy, and all exhibit broad, high-energy continuum features at 535−550 eV. As described above, it is well-established by both EHMO and ab initio calculations[14,17] that the first peak corresponds to an O 1s(C═O) → $\pi^*$(C═O) transition, where the $\pi^*$(C═O) orbitals

**TABLE 2: Experimental Energies (eV), Assignments, and Polarization Dependence for Features in the O K-Edge NEXAFS Spectra of Poly(ethylene terephthalate) (PET), Poly(butylene terephthalate) (PBT), and Its Model Compounds, 4,4′-Biphenyldicarboxylic Acid Dimethyl Ester (PAM), 4,4′-Biphenyldicarboxylic Acid (PCA), and Terephthalic Acid (TPA), and Comparison of the Assignments of Features between the Results of This Work and Those of Previous Papers[16,17]**

| | this work | | | | | | | ref 17 | | ref 16 | | |
|---|---|---|---|---|---|---|---|---|---|---|---|---|
| | energy (eV) | | | | | polarization | | energy | | energy | polarization | |
| feature | PET | PBT | PAM | PCA | TPA | dependence | assignment | (eV) | assignment | (eV) | dependence | assignment |
| a | 531.2 | 531.2 | 531.1 | 531.7 | 532.4 | $\pi$ | $\pi^*$(C═O) | 531.5 | $\pi^*$(C═O) | 532.9 | $\pi$ | $\pi^*$(C═O) |
| b | 533.5 | 533.5 | 533.6 | 533.6 | 534.1 | $\pi$ | $\pi^*$(C═O) | 534.0 | $\pi^*$(C═O) | 535.4 | $\pi$ | $\pi^*$(C═O) |
| c | 536.4 | 536.4 | 537.1 | | | $\sigma$ | $\sigma^*$(O−$CH_x$) | 536.4 | $\pi^*$(C═O, ring)), $\pi^*$(C═O) | 538.2 | no depend. | IP(C═O)[a] |
| d | 540 | 540 | 540 | 540.1 | 540.4 | $\sigma$ | $\sigma^*$(C−O) | 540.3 | $\sigma^*$(C−O) | 541.8 | $\sigma$ | $\sigma^*$(C−O) |
| e | 545.1 | 545.1 | 545.2 | 540.4 | 545.6 | $\sigma$ | $\sigma^*$(C═O) | 546 | $\sigma^*$(C═O) | 545 | $\sigma$ | $\sigma^*$(C═O) |

[a] Ionization potential of the C═O oxygen species.

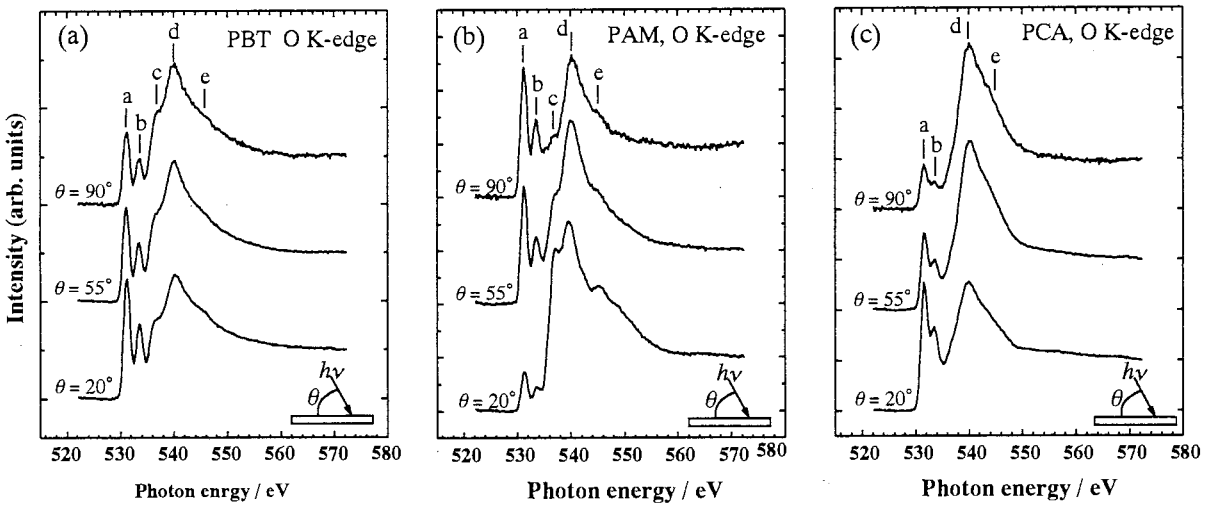


**Figure 8.** Polarization dependence of the O K-edge NEXAFS spectra of (a) PBT, (b) PAM, and (c) PCA for the X-ray incidence angle, $\theta$, relative to substrate surface.

are in the in-phase. The second peak b was assigned as the O 1s(C−O) → $\pi^*$(C═O) transition by EHMO calculation,[14] and as a combination of O 1s(C═O) → $\pi^*$(C═O) and O 1s(C−O) → $\pi^*$(C═O) transitions, where the $\pi^*$(C═O) orbitals have the out- and in-phase relationship, respectively, by ab initio calculation.[17] These assignments are consistent with the $\pi$ character deduced by the presently observed polarization dependence.

The third peak c has been assigned to an O 1s → 3p/Rydberg transition,[14] a combination of O 1s(C═O) → $\pi^*$(C═O/ring) and C 1s(C−O) → $\pi^*$(C═O) transitions by ab initio calculation,[17] and the ionization onset of the C═O oxygen.[16] Here the $\pi^*$-(C═O) transitions have the out-phase. However, the polarization dependence clearly shows that peak c is a $\sigma^*$ transition. We also note that this peak appears only in the spectra of PBT, PET, and PAM including the O−$CH_x$ bond in the ester groups. From these results, the peak c can be assigned to an O 1s → $\sigma^*$(O−$CH_x$) excitation. This assignment is also supported by the results of photon-stimulated ion desorption spectroscopy from poly(methyl methacrylate). The photon energy dependence of $CH_3^+$ ion yield shows maximum intensity at the energy corresponding to peak c in the O K-edge NEXAFS spectrum.[7,43] This excitation to the $\sigma$ antibonding state will lead to the breaking of this C−O bond.

The broad peaks d around 540 eV and e around 546 eV are clearly seen in the NEXAFS spectra of PAM at small $\theta$. They were ascribed to O 1s(C−O) → $\sigma^*$(C−O) and O 1s (C═O) → $\sigma^*$(C═O) transitions, respectively.[14,16,17] These assignments are consistent with the presently observed results, and we also adopt them.

## Conclusion

In this work, we studied poly(butylene terephthalate) (PBT), poly(ethylene terephthalate) (PET), and their model compounds 4,4′-biphenyldicarboxylic acid dimethyl ester (PAM), 4,4′-biphenyldicarboxylic acid (PCA), and terephthalic acid (TPA) by polarized near edge X-ray absorption fine structure (NEXAFS) spectroscopy. The observed spectral features of PBT and PET could be assigned in detail by the polarization dependence and the comparison among the compounds.

Some of the features were reassigned on the basis of the new experimental observations. Also we have shown that well-orientated samples of PBT, PAM, and PCA can be obtained by simple methods such as casting and vacuum evaporation, and the molecular orientation in these orientated samples could be deduced. These results have added another good example demonstrating that the polarization dependence of the NEXAFS spectra of oriented small analogues is useful for the assignments of the NEXAFS spectra of polymers, besides the more reliable assignments of the spectral features. Another point of interest was that a reasonably well-oriented sample of PBT could be prepared in contrast to the difficulty of orienting PET. This is a useful observation, since the NEXAFS spectra of these two polymers are almost identical. This suggests the possibility of developing a generally applicable technique of using chemically modifying a polymer for obtaining better oriented samples without affecting the NEXAFS spectra.

By combining the presently observed experimental results with the theoretical and experimental work by others, we could derive rather reliable spectral assignments about these polymers

of fundamental importance, although there is some ambiguity about the assignments of high-energy features. The accumulation of analyses with similar quality about other polymers will establish a sound basis for the analysis of more complex polymers.

**Acknowledgment.** We are grateful to Prof. A. P. Hitchcock of McMaster University for useful discussion. This work has been performed under the approval of the Photon Factory Advisory Committee (proposals 95G372 and 95G374). This work was supported in part by Grants-in-Aid for Scientific Research from the Ministry of Education, Science, Sports and Culture of Japan (07NP0301 and 07CE2004) and also by the Venture Business Laboratory Project "Advanced Nanoprocess Technology" of Nagoya University.

## References and Notes

(1) Stöhr, J. *NEXAFS Spectroscopy*, Springer-Verlag: Berlin, 1992.
(2) Stöhr, J.; Outka, D. A.; Baberschke, K.; Avanitis, D.; Horsley, J. A. *Phys. Rev. B* **1987**, *36*, 2976.
(3) Jordan-Sweet, J. L.; Kovac, C. A.; Goldberg, M. J.; Morar, J. F. *J. Chem. Phys.* **1988**, *89*, 2482.
(4) Ohta, T.; Seki, K.; Yokoyama, T.; Morisada, I.; Edamatsu, K. *Phys. Scr.* **1990**, *41*, 150.
(5) Ade, H.; Zhang, X.; Cameron, S.; Costello, C.; Kirz, J.; Williams, S. *Science* **1992**, *258*, 972.
(6) Kikuma, J.; Tonner, B. P. *J. Electron Spectrosc. Relat. Phenom.* **1996**, *82*, 53.
(7) Tinone, M. C. K.; Tanaka, K.; Murayama, J.; Ueno, N.; Imamura, M.; Matsubayashi, M. *J. Chem. Phys.* **1994**, *100*, 5988.
(8) Urquhart, S. G.; Hitchcock, A. P.; Leapman R. D.; Prester, R. D.; Rightor, E. G. *J. Polym. Sci.* **1995**, *33*, 1593.
(9) Urquhart, S. G.; Hitchcock, A. P.; Prester, R. D.; Rightor, E. G. *J. Polym. Sci.* **1995**, *33*, 1603.
(10) Lippitz, A.; Koprinarov, I.; Frendrich, J. F.; Unger, E. S.; Weiss, K.; Wöll, Ch. *Polymer* **1996**, *37*, 3157.
(11) Mori, I.; Araki, T.; Ishii, H.; Ouchi, Y.; Seki, K.; Kondo, K. *J. Electron Spectrosc. Relat. Phenom.* **1996**, *78*, 371.
(12) Nagayama, K.; Sei, M.; Mitsumoto, R.; Ito, E.; Araki, T.; Ishii, H.; Ouchi, Y.; Seki, K.; Kondo, K. *J. Electron Spectrosc. Relat. Phenom.* **1996**, *78*, 375.
(13) Yokoyama, T.; Seki, K.; Morisada, I.; Edamatsu, K.; Ohta, T. *Phys. Scr.* **1990**, *41*, 189.
(14) Hitchcock, A. P.; Urquhart, S. G.; Rightor, E. G. *J. Phys. Chem.* **1992**, *96*, 8736.
(15) Ouchi, I.; Nakai, I.; Kamada, M.; Tanaka, S.; Hagiwara, T. *Polym. J.* **1995**, *2*, 127.
(16) Lippitz, A.; Friedrich, J. F.; Unger, S. G.; Schertel, A.; Wöll, Ch. *Polymer* **1996**, *37*, 3151.
(17) Urquhart, S. G.; Hitchcock, A. P.; Smith, A. P.; Ade, H.; Rightor, E. G. Private communication.
(18) Patterson, L. G. M.; Ågren, H. Private communication.
(19) Warwick, T.; Ade, H.; Hitchcock, A. P.; Padmore, H.; Rightor, E. G.; Tonner, B. P. *J. Electron Spectrosc. Relat. Phenom.* **1997**, *84*, 85.
(20) Ade, H.; Smith, A. P.; Zhang, H.; Zhuang, G. R.; Kirz, J.; Rightor, E. H.; Hitchcock, A. P. *J. Electron Spectrosc. Relat. Phenom.* **1997**, *84*, 53.
(21) Koprinarov, I.; Lippitz, A.; Friedrich, J. F.; Unger, W. E. S.; Wöll, Ch. *Polymer* **1997**, *38*, 2005.
(22) Kosugi, N. *Theor. Chim. Acta* **1987**, *72*, 149.
(23) Ågren, H.; Garravetta, V.; Vatras, O.; Patterson, L. G. M. *Chem. Phys. Lett.* **1994**, *222*, 75.
(24) Rühl, E.; Hitchcock, A. P. *J. Am. Chem. Soc.* **1989**, *111*, 5069.
(25) Rühl, E.; Wen, A.; Hitchcock, A. P. *J. Electron Spectrosc. Relat. Phenom.* **1991**, *57*, 137.
(26) Wen, A.; Rühl, E.; Hitchcock, A. P. *Organometallics* **1992**, *11*, 2559.
(27) Francis J. T.; Hitchcock, A. P. *J. Phys. Chem.* **1992**, *96*, 6598.
(28) Hitchcock, A. P. *Phys. Scr.* **1990**, *T31*, 159.
(29) Stöhr, J.; Outka, D. A. *Phys. Rev. B* **1987**, *36*, 7891.
(30) Brown, F. C.; R. Z. Bachrach, R. Z.; Lien, N. *Nucl. Instrum. Methods* **1978**, *152*, 76.
(31) Yanagihara, M.; Maezawa, H.; Sasaki, T.; Ikuchi, Y. *KEK Rep.* **1984**, 84−17.
(32) King, G. C.; Tronc, M.; Read, F. H.; Bradfort, R. C. *J. Phys. B* **1977**, *10*, 2479.
(33) Sodhi, R. N.; Brion, C. E. *J. Electron Spectrosc. Relat. Phenom.* **1984**, *34*, 363.
(34) Hitchcock, A. P.; Brion, C. E. *J. Electron Spectrosc. Relat. Phenom.* **1980**, *18*, 1.
(35) Hitchcock, A. P.; Brion, C. E. *Chem. Phys.* **1978**, *33*, 55.
(36) Narioka, S.; Seki, K. Unpublished data.
(37) Stewart, J. J. P. *J. Comput. Chem.* **1989**, *10*, 209.
(38) QCPE Public Domain Software #455.
(39) Yokoyama, T.; Seki, K.; Morisada, I.; Edamatsu, K.; Ohta, T. *Phys. Scr.* **1990**, *41*, 189.
(40) Solomon, J. L.; Madix, R. J.; Stöhr, J. *Surf. Sci.* **1991**, *255*, 12.
(41) Lytle, F. W.; Greegor, R. B.; Via, G. H.; Brown, J. M.; Meitzner, G. *J. Phys.* **1986**, *C8*, 149.
(42) Hitchcock, A. P.; Brion, C. E. *J. Electron Spectrosc. Relat. Phenom.* **1980**, *19*, 231.
(43) Ueno, N.; Kamiya, K.; Harada, Y.; Tinone, M. C. K.; Sekitani, T.; Tanaka, K. *Optelectronics* **1996**, *11*, 91.